Referee #1

Overall evaluation:

This study has investigated the impact of simultaneously assimilating satellite soil moisture data from L-band SMAP, C-band ASCAT and X-band MWRI into the Common Land Model (CoLM) for improving soil moisture estimates. The impact was evaluated by comparing both spatial and temporal soil moisture patterns with in situ data from the ISMN and the CMA networks. While the results of the study are interesting, further details are needed regarding the methodologies employed and the results obtained. Additionally, some interpretations presented appear speculative and require stronger justification.

Response:

We sincerely thank you for your valuable time and professional guidance. Your comments have greatly improved the quality of this manuscript.

Following your suggestion, we further refined the description of the assimilation methodology by providing a more detailed account of key technical aspects, including the observation operator, parameter settings, construction of the observation and background error covariance matrices, quality control, and bias correction. These revisions help readers better understand the methodological framework of our study. In addition, we added descriptions of the retrieval products from different frequency bands and the quantitative evaluation strategy, which further facilitates the interpretation of the physical mechanisms underlying the assimilation performance.

To further enhance the robustness of our conclusions, we conducted additional multi-season experiments. The new results further support our conclusion that, in the assimilation application of X-band products, introducing physical constraints related to vegetation type and optimizing data screening can lead to more stable additive improvements from X-band assimilation. Moreover, through the comparative analysis of multi-season assimilation performance, we found that, in addition to vegetation type, the seasonal variation of vegetation should also be considered when assessing the impact of X-band assimilation. These additional findings further strengthen the scientific value of the manuscript.

Below, we provide a detailed point-by-point response to your comments, and the corresponding revisions in the manuscript have been highlighted in a specific color.

Major Comments:

1. The assertion that this work represents a 'paradigm shift' (Lines 414ff) is not supported by the existing literature. Numerous studies, including those conducted within the framework of the ESA CCI programme, have previously utilized complementary information from different satellite soil moisture sensors and developed dynamic weighting schemes.

Response:

Thanks for your suggestions. Following your suggestions, we have revised the relevant text in the Introduction to avoid the expression “paradigm shift”. We also added a discussion of previous multi-satellite soil moisture assimilation and merging studies, and further clarified the specific contribution of our study.

In the revised manuscript, we added a discussion of previous studies on the integration of observations from different satellites. The corresponding revision can be found in Lines 115–121 of the revised manuscript. The revised text is as follows:

"Draper et al. (2012) assimilated passive and active microwave soil moisture retrievals and reported improved estimates. Lievens et al. (2017) further combined SMAP and Sentinel-1 observations and found that the joint assimilation scheme performed best. Girotto et al. (2019) assimilated SMOS brightness temperatures together with GRACE observations, improving estimates of soil moisture, groundwater, and runoff. The ESA-CCI project has likewise explored the integration of multiple satellite retrieval products to generate more consistent and higher-quality global datasets, primarily through the development of dynamic weighting schemes based on Triple Collocation (TC) error variance estimation (Dorigo et al., 2017; Gruber et al., 2019). "

We also clarified the research background and motivation for incorporating X-band retrieval products into multi-satellite data assimilation. The corresponding revision can be found in Lines 123–129 of the revised manuscript. The revised text is as follows:

"Although data assimilation integrating observations from multiple satellites has received increasing attention, relatively few studies have focused on multi-satellite assimilation that explicitly incorporates X-band observations. China has launched several Fengyun-3 (FY-3) polar-orbiting meteorological satellites. Among the currently operating FY-3 satellites, FY-3D, FY-3F, FY-3G, and FY-3H carry microwave imagers, including MWRI/MWRI-II and MWRI-RM, with X-band channels, providing abundant retrieval products derived from X-band microwave observations. Therefore, how to effectively integrate X-band products with products from other frequency bands remains an important research direction that requires further investigation. "

We further clarified the main contribution of our study by emphasizing the specific challenge of achieving stable improvements when assimilating X-band retrieval products together with products from other frequency bands in global land data assimilation. The corresponding revision can be found in Lines 155–161 of the revised manuscript. The revised text is as follows:

"Although adjusting observation weights based on error estimation results can reduce the negative influence of highly uncertain data on assimilation performance, the relatively large errors associated with X-band products indicate that their observations may exhibit comparatively large deviations. Even when assigned small weights, such observations may still lead to degraded assimilation performance. This issue is more evident in global land data assimilation. Therefore, effectively integrating X-band retrieval products with those from other frequency bands and achieving stable improvements in global land data assimilation remain key challenges for the assimilation of X-band products. "

The following references have been added to the reference part of the revised manuscript:

Carrera, M. L., Bélair, S., and Bilodeau, B.: Assimilation of passive L-band microwave brightness temperatures in the Canadian Land Data Assimilation System: Impacts on short-range warm season numerical weather prediction, J. Hydrometeor., 20, 1085–1105, https://doi.org/10.1175/JHM-D-18-0133.1, 2019.

Dorigo, W., Wagner, W., Albergel, C., Albrecht, F., Balsamo, G., Brocca, L., Chung, D., Ertl, M., Forkel, M., Gruber, A., Haas, E., Hamer, P. D., Hirschi, M., Ikonen, J., de Jeu, R., Kidd, R., Lahoz, W., Liu, Y. Y., Miralles, D., Mistelbauer, T., Nicolai-Shaw, N., Parinussa, R., Pratola, C., Reimer,

C., van der Schalie, R., Seneviratne, S. I., Smolander, T., and Lecomte, P.: ESA CCI Soil Moisture for improved Earth system understanding: State-of-the art and future directions, Remote Sens. Environ., 203, 185–215, https://doi.org/10.1016/j.rse.2017.07.001, 2017.
Gruber, A., Scanlon, T., van der Schalie, R., Wagner, W., and Dorigo, W.: Evolution of the ESA CCI Soil Moisture climate data records and their underlying merging methodology, Earth Syst. Sci. Data, 11, 717–739, https://doi.org/10.5194/essd-11-717-2019, 2019.
Reichle, R. H., Liu, Q., Koster, R. D., Crow, W. T., De Lannoy, G. J. M., Kimball, J. S., Ardizzone, J. V., Bosch, D., Colliander, A., Cosh, M., Kolassa, J., Mahanama, S. P., Prueger, J., Starks, P., and Walker, J. P.: Version 4 of the SMAP Level-4 Soil Moisture Algorithm and Data Product, J. Adv. Model. Earth Syst., 11, 3106–3130, https://doi.org/10.1029/2019MS001729, 2019.

The following references are cited here and were already included in the original manuscript:

Tian, J., Lu, H., Yang, K., Qin, J., Zhao, L., Zhou, J., Jiang, Y., and Ma, X.: Quick estimation of parameters for the land surface data assimilation system and its influence based on the extended Kalman filter and automatic differentiation, Sci. China Earth Sci., 66, 2546–2562, https://doi.org/10.1007/s11430-022-1180-8, 2023.

2. The authors do not properly describe active and passive microwave sensors, and their specifications and characteristics. Most importantly, differences in the performance of the products cannot merely be explained by differences in frequency given that SMAP and MWRI are passive sensors and ASCAT is an active sensor. This leads to wrong statements and interpretations.

Response：

Thanks for your suggestions. Following your suggestions, we revised the relevant paragraph in the Introduction. In the revised manuscript, we provide a more detailed description of active and passive microwave sensors, their respective frequency bands, and their interactions with land surface features, such as topography and vegetation. We also clarify the physical mechanisms underlying the differences in retrieval performance among different sensors. The detailed responses to this comment are provided below.

2a. On line 72 they write: "Active microwave sensors offer finer resolution but lower temporal sampling due to long revisit periods." This is only true for SAR, but not scatterometers.

Response：

Thanks for your suggestions. Following your suggestions, we revised the relevant paragraph in the Introduction to provide a clearer description of the characteristics of different microwave sensors, especially the classification within active microwave sensors. The revised text distinguishes among SAR products, ASCAT products, and SMAP products, and further clarifies their differences in spatial resolution and temporal coverage. The corresponding revision can be found in Lines 81–88 of the revised manuscript. The revised text is as follows:

"Depending on the instrument bands and orbital characteristics, the strengths and weaknesses of various soil moisture products differ significantly. Passive microwave products offer excellent temporal coverage but suffer from coarse spatial resolution. Conversely, while Synthetic Aperture Radar (SAR) products provide high spatial resolution, their temporal coverage is limited. The Scatterometer (ASCAT) strikes a balance with high temporal coverage and moderate resolution, while L-band active-passive combined instruments, such as SMAP, attempt to integrate the advantages of all three. Although continuous advancements in retrieval algorithms have led to marked improvements in the accuracy of soil moisture products across all instrument types, vegetation density continues to exert a significant influence on the product precision of instruments operating in different frequency bands."

2b. Line 75: "L-band missions (SMOS, SMAP) penetrate vegetation well but exhibit larger errors over complex terrain." Complex terrain is challenging for all microwave sensors, but certainly even more problematic for active than passive sensors.

Response：

Thanks for your suggestions. Following your suggestions, we revised the relevant text in the Introduction to more accurately describe the influence of complex terrain on microwave observations. We also added the physical mechanisms responsible for the stronger impact of complex terrain on active microwave sensors, particularly SAR. The corresponding revision can be found in Lines 104–107 of the revised manuscript. The revised text is as follows:

"Furthermore, retrieval accuracy is influenced by environmental factors. Although complex terrain poses a universal challenge to all microwave observations, its impact on active microwave sensors, particularly SAR, is more severe because of their high sensitivity to local incidence angle variations and geometric distortions."

In addition, we revised the description of L-band sensors to clarify both their penetration capability and their limitations under dense vegetation conditions. The corresponding revision can be found in Lines 97–100 of the revised manuscript. The revised text is as follows:

"Compared with high-frequency bands, L-band sensors such as SMOS and SMAP possess superior physical penetration capabilities, which allow them to effectively penetrate the vegetation canopy and acquire soil information. However, in regions with dense vegetation cover, specifically when the vegetation water content (VWC) exceeds 5 kg/m², the capacity to effectively retrieve surface information remains significantly limited (Entekhabi et al., 2010; Kerr et al., 2010)."

The following references have been added to the reference part of the revised manuscript:

Kerr, Y. H., Waldteufel, P., Wigneron, J.-P., Delwart, S., Cabot, F., Boutin, J., Escorihuela, M.-J., Font, J., Reul, N., Gruhier, C., Juglea, S. E., Drinkwater, M. R., Hahne, A., Martín-Neira, M., and Mecklenburg, S.: The SMOS Mission: New Tool for Monitoring Key Elements ofthe Global Water Cycle, Proc. IEEE, 98, 666–687, https://doi.org/10.1109/JPROC.2010.2043032, 2010.

The following references are cited here and were already included in the original manuscript:

Entekhabi, D., Njoku, E. G., O'Neill, P. E., Kellogg, K. H., Crow, W. T., Edelstein, W. N., Entin, J. K., Goodman, S. D., Jackson, T. J., Johnson, J., Kimball, J., Piepmeier, J. R., Koster, R. D., Martin, N., McDonald, K. C., Moghaddam, M., Moran, S., Reichle, R., Shi, J. C., Spencer, M. W., Thurman, S. W., Tsang, L., and Van Zyl, J.: The Soil Moisture Active Passive (SMAP) Mission, Proc. IEEE, 98, 704–716, https://doi.org/10.1109/JPROC.2010.2043918, 2010.

2c. Line 76: "C-band sensors (ASCAT, Sentinel-1) have high temporal resolution but variable accuracy across vegetation types and seasons." Only ASCAT has a high temporal resolution, not Sentinel-1. One can note that – while it is true that the accuracy varies by vegetation type and season – this is nothing unique for active sensors. The same applies of course for passive sensors.

Response：

Thanks for your suggestions. Following your suggestions, we revised the Introduction to avoid presenting Sentinel-1 and ASCAT as having similar temporal resolution. We also reorganized the discussion of differences among frequency bands and clarified the specific advantages of active C-band sensors such as ASCAT. The corresponding revision can be found in Lines 100–104 of the revised manuscript. The revised text is as follows:

"Compared with longer wavelengths, C-band observations generally exhibit limited vegetation penetration capabilities. Nevertheless, the ASCAT scatterometer benefits from its multi-incidence-angle viewing geometry and a change-detection algorithm that relies on long-term time series. These features enable reliable detection of soil moisture dynamics in regions with moderate vegetation density and relatively slow vegetation changes (Wagner et al., 2013; Chen et al., 2018)."

The following references are cited here and were already included in the original manuscript:

Chen, F., Crow, W. T., Bindlish, R., Colliander, A., Burgin, M. S., Asanuma, J., and Aida, K.: Global-scale evaluation of SMAP, SMOS and ASCAT soil moisture products using triple collocation, Remote Sens. Environ., 214, 1–13, https://doi.org/10.1016/j.rse.2018.05.008, 2018.

Wagner, W., Hahn, S., Kidd, R., Melzer, T., Bartalis, Z., Hasenauer, S., Figa-Saldana, J., de Rosnay, P., Jann, A., Schneider, S., Komma, J., Kubu, G., Brugger, K., Aubrecht, C., Züger, J., Gangkofner, U., Kienberger, S., Brocca, L., Wang, Y., Blöschl, G., Eitzinger, J., Steinnocher, K., Zeil, P., and Rubel, F.: The ASCAT soil moisture product: a review of its specifications, validation results, and emerging applications, Meteorol. Z., https://doi.org/10.1127/0941-2948/2013/0399, 2013.

2d. Line 90: "L-band sensors penetrate vegetation well and perform best in moderately vegetated areas; C-band sensors have moderate penetration and are sensitive to vegetation changes; X-band sensors have weak penetration and mainly capture near-surface signals." This description is oversimplified and partly not true, e.g. ASCAT can be better than SMAP over moderately vegetated areas.

Response：

Thanks for your suggestions. Following your suggestions, we revised the relevant

section to avoid evaluating soil moisture retrieval performance solely based on microwave frequency bands. We removed the previous band-based classification and reorganized the discussion around representative sensors, including SMAP, ASCAT, and MWRI. The revised discussion compares their observational characteristics and retrieval performance under different vegetation density conditions. The corresponding revision can be found in Lines 139–153 of the revised manuscript. The revised text is as follows:

"Under sparse vegetation or bare soil conditions, microwave attenuation by the vegetation canopy is typically minimal. Consequently, L-band (e.g., SMAP), C-band (e.g., ASCAT), and X-band (e.g., FY-3 MWRI) sensors all exhibit high sensitivity to variations in near-surface soil moisture (Jackson and Schmugge, 1991). In regions with low to moderate vegetation density, such as croplands and grasslands, vegetation scattering and attenuation begin to affect microwave signals. Although L-band sensors generally provide superior vegetation penetration, ASCAT can still achieve stable soil moisture retrieval accuracy in many of these areas, owing to its multi-angle viewing geometries and time-series-based change detection algorithms. In high-density vegetation regions such as forests, scattering and attenuation become dominant, causing a pronounced loss of shorter wavelength bands, specifically C-band and higher frequencies, to soil moisture (Owe et al., 2001). While C-band products require external vegetation corrections, L-band instruments typically retain better (though still limited) retrieval performance when VWC remains below 5 kg/m^2 (Kerr et al., 2010; Kim et al., 2018). In contrast, the shorter wavelength of FY-3 MWRI makes it more sensitive to vegetation structure changes, resulting in greater accuracy fluctuations across vegetation gradients. MWRI products can therefore serve as a useful supplement in sparse vegetation or bare soil areas where L- and C-band coverage is insufficient; however, in moderate to dense vegetation, their lower accuracy limits their utility for land surface data assimilation (Yao et al., 2023)."

The following references have also been added to the revised manuscript:

Yao, P., Lu, H., Zhao, T., Wu, S., Peng, Z., Cosh, M. H., Jia, L., Yang, K., Zhang, P., and Shi, J.: A global daily soil moisture dataset derived from Chinese FengYun Microwave Radiation Imager (MWRI) (2010–2019), Sci. Data, 10, 133, https://doi.org/10.1038/s41597-023-02007-3, 2023.

The following references are cited here and were already included in the original manuscript:

Jackson, T. J. and Schmugge, T. J.: Vegetation effects on the microwave emission of soils, Remote Sens. Environ., 36, 203–212, https://doi.org/10.1016/0034-4257(91)90057-D, 1991.

Kerr, Y. H., Waldteufel, P., Wigneron, J.-P., Delwart, S., Cabot, F., Boutin, J., Escorihuela, M.-J., Font, J., Reul, N., Gruhier, C., Juglea, S. E., Drinkwater, M. R., Hahne, A., Martín-Neira, M., and Mecklenburg, S.: The SMOS Mission: New Tool for Monitoring Key Elements ofthe Global Water Cycle, Proc. IEEE, 98, 666–687, https://doi.org/10.1109/JPROC.2010.2043032, 2010.

Kim, H., Parinussa, R., Konings, A. G., Wagner, W., Cosh, M. H., Lakshmi, V., Zohaib, M., and Choi, M.: Global-scale assessment and combination of SMAP with ASCAT (active) and AMSR2 (passive) soil moisture products, Remote Sens. Environ., 204, 260–275, https://doi.org/10.1016/j.rse.2017.10.026, 2018.

Owe, M., de Jeu, R., and Walker, J.: A methodology for surface soil moisture and vegetation optical depth retrieval using the microwave polarization difference index, IEEE Trans. Geosci. Remote Sens., 39, 1643–1654, https://doi.org/10.1109/36.942542, 2001.

3. There are some choices made in the assimilation (Section 3.3) which need much better justification than merely citing past research.

Response：

Thanks for your suggestions. Following your suggestions, we revised the “SEKF assimilation system” section (Section 3.3) to provide a more detailed explanation of the assimilation setup. The revised text clarifies the rationale behind the perturbation strategy and the vertical mapping used in the assimilation procedure. The detailed responses to this comment are provided below.

3a. There is no logic in the selected pertubations for the different layers. Explain.

Response：

Thanks for your suggestions. Following your suggestions, we added Figure R1 and conducted additional sensitivity experiments to support the selection of perturbation magnitudes. The selection rationale and experimental procedure are described in the “SEKF assimilation system” section (Section 3.3) as follows:

"According to the limit definition of the derivative, the derivative of a function can be approximated via the finite difference method. For any given model grid point, the first-order derivative of the observation operator can thus be calculated by introducing a small perturbation to the independent variable. As the perturbation amplitude becomes sufficiently small, the difference between the perturbed and unperturbed function values of the observation operator approximates its first-order derivative. To identify a sufficiently small perturbation, the right derivative $\mathbf{H}^{+}$ and left derivative $\mathbf{H}^{-}$ are evaluated and compared. When the discrepancy between $\mathbf{H}^{+}$ and $\mathbf{H}^{-}$ approaches zero, their mean value is adopted as the first-order derivative of the observation operator at the corresponding grid point (Balsamo et al., 2007). To minimize the influence of meteorological variability, we calculated globally averaged derivatives over all grid points under different perturbation magnitudes (Figure R1). As an example, for the second soil layer (Figure R1b), a perturbation of 10^{-3} m^3/m^3 produced a stable derivative of approximately 0.35, while the difference between $\mathbf{H}^{+}$ and $\mathbf{H}^{-}$ is close to zero. Based on this criterion, the optimal perturbation values for the first seven soil layers are selected as 0.001, 0.0001, 0.0001, 0.0001, 0.0005, 0.001, and 0.0005 m^3/m^3, respectively."

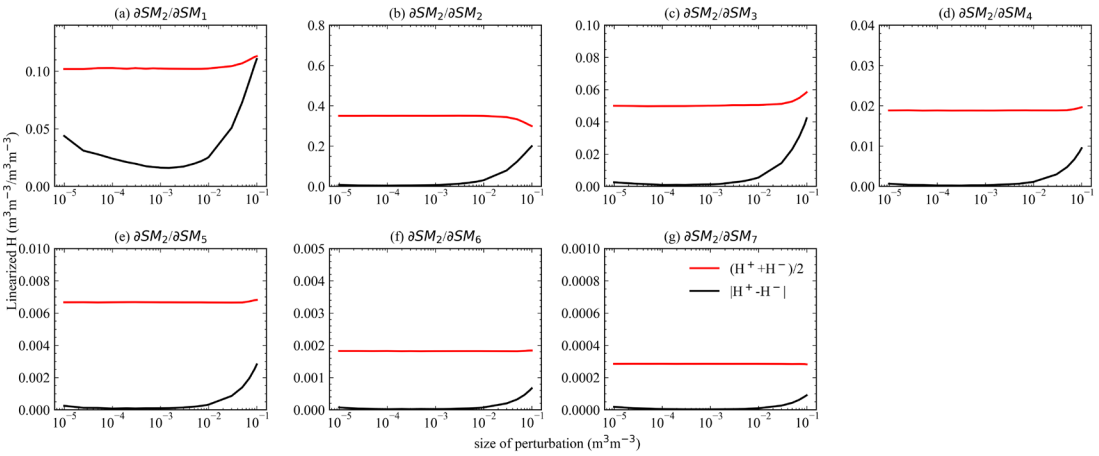

Figure R1: The $\partial SM_2/\partial SM_n$ characteristics with respect to size of perturbation in different layers are shown. The black line represents $|H^{+}-H^{-}|$, and the red line represents $(H^{+}+H^{-})/2$.

The following references are cited here and were already included in the original manuscript:

Balsamo, G., Mahfouf, J.-F., Bélair, S., and Deblonde, G.: A Land Data Assimilation System for Soil Moisture and Temperature: An Information Content Study, J. Hydrometeorol., 8, 1225–1242, https://doi.org/10.1175/2007JHM819.1, 2007.

b. The authors state that the satellite soil moisture data are mapped into the second layer (7-28 cm). This counter intuitive given that the satellite data match much closer to the first layer (0-7 cm).

Response:

We apologize that this point may have given the impression that the second layer referred to here corresponds to the second soil layer of ERA5-Land. In the revised manuscript, we clarified that this layer refers specifically to the second soil layer of CoLM. The corresponding revision can be found in Lines 227–233 of the revised manuscript. The added text is as follows:

Specifically, satellite-derived soil moisture was matched to the CoLM background simulations for summer 2022 and then mapped to the model's second soil layer, consistent with Albergel et al. (2017). This layer was selected because it better matches the effective sensing depth of the satellite products. In this CoLM setup, the top layer is 0–1.75 cm thick and responds quickly to rainfall, evaporation, and surface thermal forcing, so it mainly captures short-lived surface fluctuations. The second layer, which spans 1.75–4.51 cm, is closer to the main sensing depth of SMAP and ASCAT (about 0–5 cm) and provides a more stable representation of near-surface soil moisture. It was therefore used for observation mapping and bias correction.

The following references are cited here and were already included in the original manuscript:

Albergel, C., Munier, S., Leroux, D. J., Dewaele, H., Fairbairn, D., Barbu, A. L., Gelati, E., Dorigo, W., Faroux, S., Meurey, C., Le Moigne, P., Decharme, B., Mahfouf, J.-F., and Calvet, J.-C.: Sequential assimilation of satellite-derived vegetation and soil moisture products using SURFEX_v8.0: LDAS-Monde assessment over the Euro-Mediterranean area, Geosci. Model Dev., 10, 3889–3912, https://doi.org/10.5194/gmd-10-3889-2017, 2017.

4. The evaluation methods are not adequately described. For example, it is not fully clear what how the spatial correlation coefficients (R) and root-mean-square error (RMSE) relative ERA5-Land, shown in Figure 2, are calculated.

Response:

Thanks for your suggestions. Following your suggestions, we added a dedicated section on the evaluation methods in the revised manuscript (Section 3.5). This section provides the complete formulas for the evaluation metrics and gives a more detailed description of the statistical procedures.

In addition, before presenting each evaluation result, we clarified how these metrics were calculated for the corresponding analysis. These clarifications can be found in Lines 403, 447, 471, and 496 of the revised manuscript. For the global analysis shown in Figure 5, R and RMSE are computed separately for each soil layer and each time step, using all available global land grid cells and taking ERA5-Land as the reference. For the analyses by latitudinal band and vegetation type, the same procedure is applied, but only to the land grid cells within each latitudinal band (Figure 7) or representative vegetation type (Figure 8). The resulting time-step metrics are then averaged over the respective evaluation period. For the in situ evaluation using observations from the ISMN and CMA networks, R and RMSE are calculated from the time series of simulated and observed soil moisture at each station over the assimilation period, and the results are subsequently grouped by vegetation type (Figure 9).

5. The interpretation of why L-band assimilation decays more rapidly is extremely speculative (lines 298ff: "While L-band performs best in regions with dense vegetation and high precipitation (Mousa and Shu, 2020), soil moisture in these areas is frequently influenced by strong meteorological forcings such as rainfall. As a result, the assimilated information is more likely to be masked by subsequent hydrometeorological variability, leading to faster loss of forecast skill.") Please provide evidences that can support this interpretation.

Response：

Thanks for your suggestions. We added Figure R2 to the revised manuscript as Figure 11, together with the related discussion, to illustrate how external forcing, particularly precipitation, can mask the impact of data assimilation. The corresponding revision can be found in Lines 537–548 of the revised manuscript. The added text is as follows:

Figure R2 illustrates the impact of precipitation on the persistence of assimilation increments. Figure R2a uses a typical BET Tropical grid point (6.38°N, 59.06°W) as an example to present the soil moisture time series. During the assimilation phase, continuous observational constraints result in a distinct divergence between the soil moisture sequences of the Data Assimilation (DA) experiment and the Control (CTL) experiment. However, in the forecast phase, external forcings such as heavy precipitation dominate the soil moisture state. This causes the DA and CTL simulation results to rapidly converge, which makes the information introduced via assimilation more susceptible to being masked. Figure R2b further demonstrates that densely vegetated regions, including BET Tropical and NET Temperate, typically experience higher average precipitation. Consequently, in these regions where the assimilation of L-band retrieval products otherwise performs relatively well, frequent and intense precipitation acts as an external forcing that quickly obscures the initial assimilation information, resulting in a more rapid decay in forecast skill.

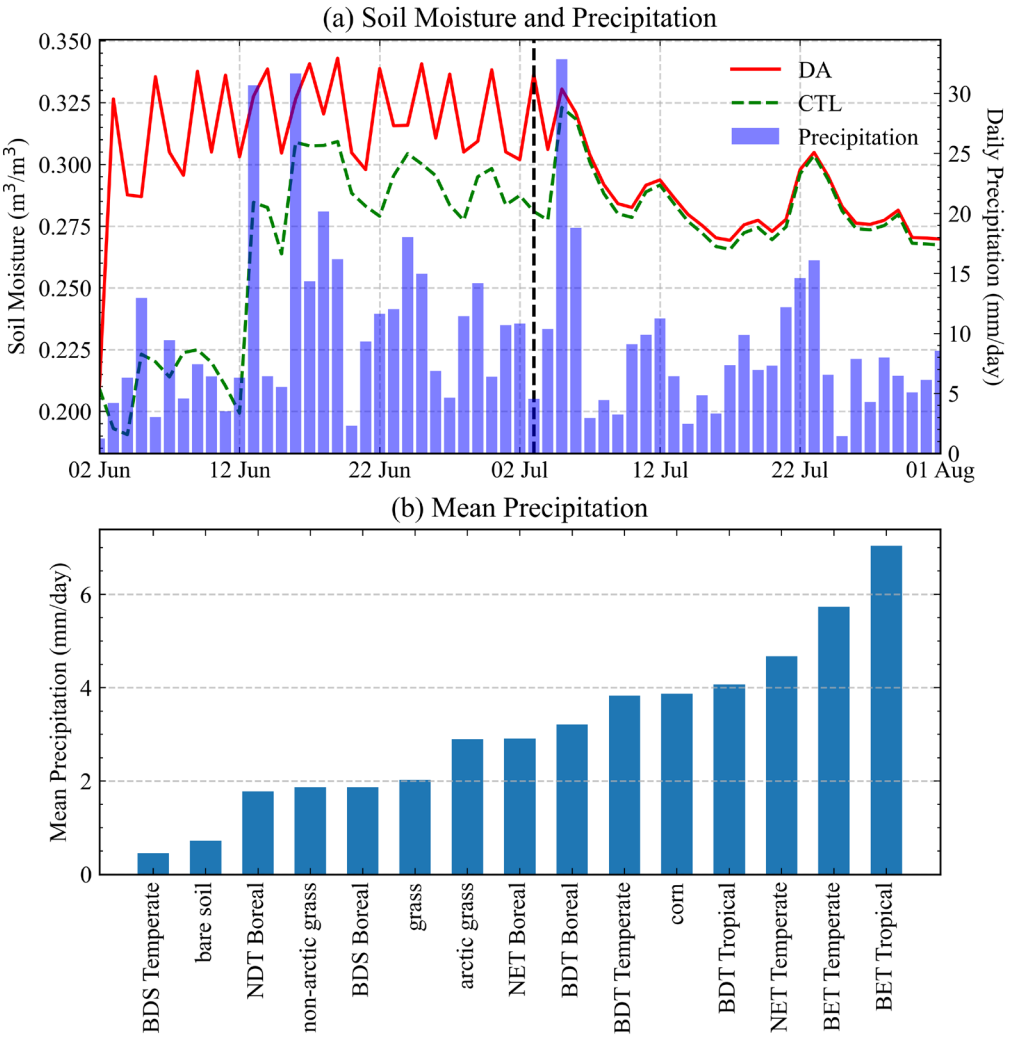

Figure R2: (a) Time series of daily precipitation and simulated soil moisture from the data assimilation (DA) and CTL experiments at a representative BET Tropical grid cell (6.38°N, 59.06°W). The vertical dashed line separates the assimilation phase and the forecast phase. (b) Mean precipitation across different vegetation types during the study period.

6. The statement (Lines 301) that "In contrast, C- and X-band retrievals perform better in regions with low-to-moderate vegetation cover and more arid conditions." is not fully correct. For ASCAT, it is known that subsurface scattering effects degrade the quality of the data in arid region.

Response:

Thanks for your suggestions. Following your suggestions, we removed this statement and reorganized the relevant paragraph to more clearly describe the improvement in assimilation performance. In addition, we added a discussion of the potential influence of subsurface scattering effects in arid regions on retrieval

performance. The corresponding revision can be found in Lines 551–557 of the revised manuscript. The added text is as follows:

"Based on the statistical results, the assimilation of C band and X band products led to improvements in assimilation performance in regions with low to moderate vegetation cover. However, it should be emphasized that such assimilation systems improve background field accuracy from a probabilistic perspective, which does not necessarily imply that the original satellite retrieval products themselves possess high precision. For active microwave sensors such as ASCAT, the penetration depth of radar signals increases significantly under extremely dry soil conditions, which triggers subsurface volume scattering effects and impacts the data quality of the soil moisture retrieval products (Wagner et al., 2013)."

The following references have been added to the revised manuscript:

Wagner, W., Hahn, S., Kidd, R., Melzer, T., Bartalis, Z., Hasenauer, S., Figa-Saldana, J., de Rosnay, P., Jann, A., Schneider, S., Komma, J., Kubu, G., Brugger, K., Aubrecht, C., Züger, J., Gangkofner, U., Kienberger, S., Brocca, L., Wang, Y., Blöschl, G., Eitzinger, J., Steinnocher, K., Zeil, P., and Rubel, F.: The ASCAT soil moisture product: a review of its specifications, validation results, and emerging applications, Meteorol. Z., https://doi.org/10.1127/0941-2948/2013/0399, 2013.

7. The statement that "L-band performs well in densely vegetated areas, …" (Line 315) is highly problematic as also L-band cannot sense soil moisture below dense forests.

Response:

Thanks for your suggestions. Following your suggestions, we reorganized this paragraph to clarify that L-band performs only relatively better than higher-frequency bands, such as C- and X-bands, under such conditions. We also noted that all existing frequency bands face inherent physical limitations in densely vegetated regions, resulting in degraded product accuracy. The corresponding revision can be found in Lines 574–579 of the revised manuscript. The revised text is as follows:

Due to its longer wavelength, the L band possesses a relatively stronger penetration capability through the vegetation canopy. Consequently, in regions with denser vegetation cover, the assimilation of L band products demonstrates relatively better performance than the assimilation of C band and X band products. However, in

regions with extremely high vegetation cover, such as dense forests, the thickness of the canopy and the high-water content within the vegetation absorb and scatter microwave signals, resulting in a decline in the quality of all soil moisture retrieval products.

8. Considering the very small differences shown in Figure 11, it is hard to agree with the statement "the NEW experiment exhibits notably better performance" (Line 372).

Response:

Thanks for your suggestions. Following your suggestions, we revised this statement to provide a more objective description of the DA_NEW experiment. The corresponding revision can be found in Line 670 of the revised manuscript. The revised statement is as follows:

"The DA_NEW experiment demonstrates a slight but constant improvement in performance."

In addition, we have added the following clarification in the revised manuscript (Lines 675–678):

"Although the magnitude of the enhancement is limited at this stage, this positive effect provides a preliminary validation of the potential of the synergistic assimilation scheme. This indicates that exploring the synergistic assimilation mechanisms of data from multiple sources can bring positive benefits to the model, representing a direction that warrants continued effort for the further optimization of soil moisture assimilation systems."

Minor Comments:

1. Section 2.1 must be much improved, providing more details about each data set used.

Response:

Thanks for your suggestions. Following your suggestions, we expanded Section 2.1 "Satellite datasets" by adding key technical and physical information on the satellite retrieval products, including their operating frequency bands, local equatorial overpass

times for ascending and descending orbits, and retrieval algorithms. The added text can be found in Lines 178–209 of the revised manuscript, as follows:

"This study utilized the Soil Moisture Active Passive (SMAP) Level-2 Enhanced Passive Soil Moisture product (L2_SM_P_E) provided by the U.S. National Snow and Ice Data Center (NSIDC) (O'Neill et al., 2023). Launched in January 2015, the SMAP satellite has been continuously providing global radiometer observations since April 2015. It operates in a sun-synchronous orbit with an L-band (1.41 GHz) radiometer. The descending and ascending overpasses occur at approximately 6:00 AM and 6:00 PM Local Solar Time, respectively, yielding a global revisit time of 2–3 days. Based on the well-validated $\tau - \omega$ radiative transfer model, this product implements both the Single Channel Algorithm using vertical polarization (SCA-V) and the Dual Channel Algorithm (DCA) for soil moisture retrieval (Chaubell et al., 2020; O'Neill et al., 2021). The characteristics of the L-band provide it with canopy penetration capabilities. Although the native spatial resolution of the radiometer is approximately 36 km, this enhanced product utilizes the Backus-Gilbert optimal interpolation technique to be distributed at a spatial sampling of 9 km on the EASE-Grid 2.0 projection.

The ASCAT retrieval data are derived from the Advanced Scatterometer onboard the MetOp-C satellite operated by the European Organization for the Exploitation of Meteorological Satellites (EUMETSAT). Following its launch in November 2018, MetOp-C has continuously provided high-quality global data, extending the long-term ASCAT data record. The satellite has equatorial crossing times of approximately 9:30 AM (descending) and 9:30 PM (ascending), providing a global revisit time of about 3 days. As an active microwave radar operating at the C-band (5.255 GHz, VV polarization), ASCAT provides global soil moisture estimates by measuring the surface radar backscatter coefficient (σ^0). This study utilizes the ASCAT Level 2 Surface Soil Moisture product (EO:EUM:DAT:METOP:SOMO12) at 12.5 km spatial sampling on the swath grid. The temporal resolution of this product relies on daily morning and evening discrete observations. Regarding the retrieval algorithm, this product is based on the TU Wien change detection algorithm, obtaining relative soil moisture, which is expressed as a degree of saturation percentage from 0 to 100%, by linearly scaling the

backscatter coefficient between historical dry and wet reference lines (Bartalis et al., 2007). Subsequently, this study utilizes soil porosity data provided by the European Space Agency Climate Change Initiative (ESA-CCI) to convert this saturation into volumetric soil water content.

The MWRI soil moisture dataset was developed by the National Satellite Meteorological Center (NSMC) of the China Meteorological Administration (CMA). The FY-3D afternoon satellite was successfully launched in November 2017, with its MWRI data record officially available since early 2018. The dataset is derived from global passive microwave brightness temperature observations acquired by the MWRI instrument onboard FY-3D, which has equatorial crossing times of approximately 2:00 AM (descending orbit) and 2:00 PM (ascending orbit), providing a global revisit time of 1–2 days. Surface soil moisture is primarily retrieved from the X-band (10.65 GHz) dual-polarized brightness temperatures using a parameterized Q_p emission model that accounts for vegetation scattering, optical depth, and soil surface roughness effects (Kang et al., 2020). This daily product combines ascending and descending overpasses and is provided on a 25 km Equal-Area Scalable Earth (EASE-Grid) projection."

The following references have also been added to the revised manuscript:

Chaubell, M. J., Yueh, S. H., Dunbar, R. S., Colliander, A., Chen, F., Chan, S. K., Entekhabi, D., Bindlish, R., O'Neill, P. E., Asanuma, J., Berg, A. A., Bosch, D. D., Caldwell, T., Cosh, M. H., Holifield Collins, C., Martínez-Fernández, J., Seyfried, M., Starks, P. J., Su, Z., Thibeault, M., and Walker, J.: Improved SMAP dual-channel algorithm for the retrieval of soil moisture, IEEE Trans. Geosci. Remote Sens., 58, 3894–3905, https://doi.org/10.1109/TGRS.2019.2959239, 2019.

O'Neill, P. E., Bindlish, R., Chan, S., Chaubell, J., Colliander, A., Njoku, E., and Jackson, T.: Soil Moisture Active Passive (SMAP) Algorithm Theoretical Basis Document: Level 2 & 3 Soil Moisture (Passive) Data Products, Revision G, Jet Propulsion Laboratory, California Institute of Technology, JPL D-66480, 111 pp., 2021.

The following references are cited here and were already included in the original manuscript:

Bartalis, Z., Wagner, W., Naeimi, V., Hasenauer, S., Scipal, K., Bonekamp, H., Figa, J., and Anderson, C.: Initial soil moisture retrievals from the METOP-A Advanced Scatterometer (ASCAT), Geophys. Res. Lett., 34, https://doi.org/10.1029/2007GL031088, 2007.

Kang, C. S., Zhao, T., Shi, J., Cosh, M. H., Chen, Y., Starks, P. J., Collins, C. H., Wu, S., Sun, R., and Zheng, J.: Global Soil Moisture Retrievals from the Chinese FY-3D Microwave Radiation Imager, IEEE Trans. Geosci. Remote Sens., 59, 4018–4032, https://doi.org/10.1109/TGRS.2020.3019408, 2020.

O'Neill, P., Chan, S., Njoku, E., Jackson, T., Bindlish, R., Chaubell, J., and Colliander, A.: SMAP enhanced L2 radiometer half-orbit 9 km EASE-grid soil moisture, version 6, https://doi.org/10.5067/BN36FXOMMC4C, 2023.

2. Section 2.1. Distinguish between spatial sampling and spatial resolution! E.g., the 12.5 km for ASCAT refer to the spatial sampling, not the spatial resolution (which is 25 km).

Response:

Thanks for your suggestions. We have carefully reviewed and corrected the relevant terminology throughout the revised manuscript, replacing ASCAT's "12.5 km spatial resolution" with "12.5 km spatial sampling."

3. Section 2.2: Show a map with the location of the ISMN and CMA in situ stations.

Response:

Thanks for your suggestions. We have added Figure R3 to the revised manuscript as Figure 2 to show the spatial distribution of the in-situ stations in Section 2.2. The added text (Lines 255–264) reads as follows:

A total of 3057 stations remained after these quality control procedures. Figure R3 illustrates the spatial distribution of the CMA and ISMN in-situ stations to provide a clear visualization of the ground-based data coverage. Among these, 2792 CMA stations are densely distributed across most of China as shown in Figure R3a. Additionally, a total of 265 ISMN stations were utilized, with the majority located in the United States and others distributed across Europe and Africa. Given that the highest station density occurs in the U.S. region, Figure R3b primarily highlights the distribution of ISMN stations in that area.

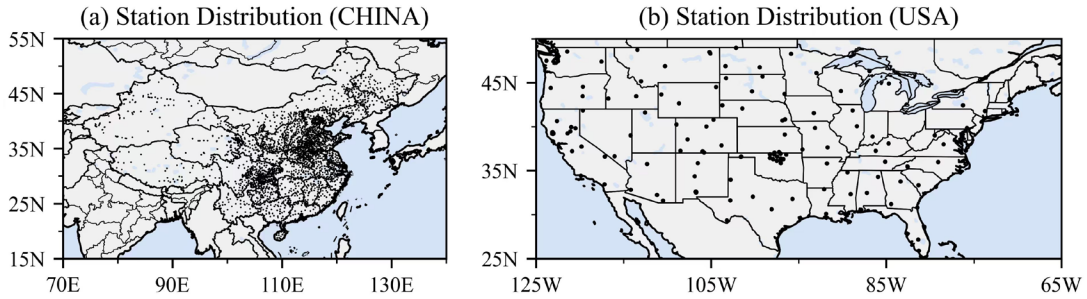

Figure R3: Spatial distribution of the in-situ soil moisture stations. (a) China Meteorological Administration network, and (b) International Soil Moisture Network stations located in the United States.

4. Section 2.2: Specify how many ISMN and CMA stations were used in the study.

Response：

Thanks for your suggestions. We have now included the specific number of stations used in Section 2.2 of the revised manuscript. Specifically, a total of 2792 CMA stations and 265 ISMN stations were selected for this study. For further details regarding these modifications, please refer to our response to Comment 3.

5. Figure 5: Not all names of vegetation types are self-evident. Describe.

Response：

Thanks for your suggestions. We have added a new table (Table 1) in the revised manuscript (Line 376) to provide the full names for all vegetation type abbreviations used in this study.

Table 1. Vegetation types

Abbreviation	Type
BDS Temperate	Broadleaf deciduous temperate shrub
NDT Boreal	Needleleaf deciduous boreal tree
BDS Boreal	Broadleaf deciduous boreal shrub
NET Boreal	Needleleaf evergreen boreal tree
BDT Boreal	Broadleaf deciduous boreal tree
BDT Temperate	Broadleaf deciduous temperate tree
BDT Tropical	Broadleaf deciduous tropical tree
NET Temperate	Needleleaf evergreen temperate tree
BET Temperate	Broadleaf evergreen temperate tree
BET Tropical	Broadleaf evergreen tropical tree

6. Figure 9: Not clear what is shown. E.g. which sensor is R-single referring to?

Response:

Thanks for your suggestions. We apologize for any confusion caused by the inaccurate labeling in Figure 9. This figure illustrates the changes resulting from the addition of a third satellite product to any given "dual-product assimilation

combination" (denoted here as R_{all}-R_{double}, the label "all" denotes the simultaneous assimilation of L-band, C-band, and X-band data, while "double" refers to the assimilation of only two of them, which can be either L and C, L and X, or C and X).

In the revised manuscript, we have corrected the X-axis tick labels in Figure 9 to rectify the erroneous descriptions. The updated figure has been integrated into the text and is also provided here as Figure R4 for your convenience.

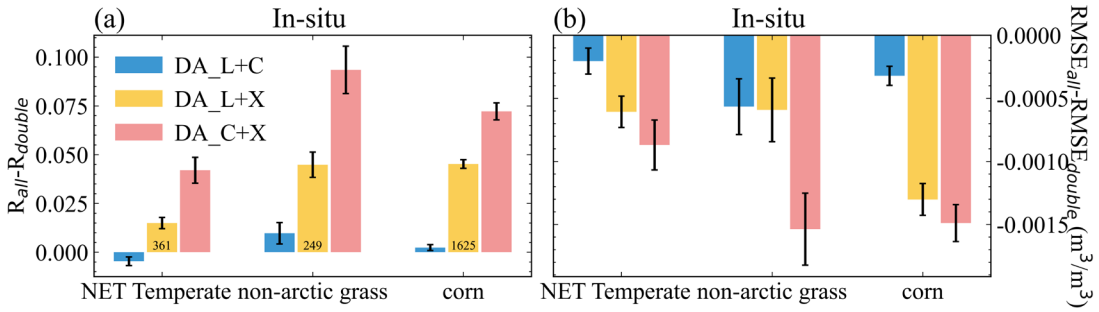

Figure R4: Changes in correlation coefficient (a) and RMSE (b) between model output and in situ observations after adding a third satellite product to each two-product assimilation combination, shown for selected vegetation types. Error bars denote 95% confidence intervals, and numbers below represent the sample size, which is identical across all groups. The label "all" denotes the simultaneous assimilation of L-band, C-band, and X-band data, while "double" refers to the assimilation of only two of them, which can be either L and C, L and X, or C and X.